

Review

Theoretical elastic behaviour of crystals at large strains

FREDERICK MILSTEIN

Department of Mechanical and Environmental Engineering, University of California, Santa Barbara, California 93106, USA

Current knowledge in the subject of the theoretical mechanical behaviour of perfect single crystals under load is reviewed. Examples of computations of load, lattice deformation, elastic moduli, and elastic stability are discussed, and qualitatively interesting (and sometimes surprising) phenomena are noted. Although computational techniques are reviewed briefly, the emphasis is upon the collation and interpretation of various computational results that have appeared in the literature. Special consideration is given to the topics of lattice stability and the definition and computation of elastic moduli of crystals under load, as well as branching from one path of deformation to another under a prescribed mode of loading. Possible applications in materials science include deformation of whiskers, twinning, martensitic transformations, very rapid shock deformation, powder technology and size reduction, and mechanical properties of small structures such as metallized integrated circuits.

1. Introduction

This article reviews current knowledge in the subject of the theoretical mechanical behaviour of perfect single crystals under load. Applications of particular interest are to systems in which large, elastic (but not necessarily linear) deformation may occur, i.e. in cases where large deformations may occur either without significant dislocation movement or before deformation by dislocation movement becomes dominant. Relevant examples may include (i) deformation of whiskers, (ii) twinning, (iii) martensitic transformations, (iv) very rapid shock deformation (e.g. if the rate of deformation is greater than the dislocation velocity), (v) powder technology and size reduction (e.g. the "theoretical strength" of solids forms a basis for calculating the efficiency of grinding processes [1]), and (vi) perhaps even mechanical properties of small structures such as metallized integrated circuit structures (presuming that regions relatively free of defects can occur).

According to Hill [2], "Single crystals free from lattice imperfections are used increasingly as micro-structural components. Perfect crystals are capable of elastic strains well beyond what can

properly be treated as infinitesimal. Their response to general loading is virtually unknown and is doubtless complex, so experimentation will have to be conducted within some plausible theoretical framework". As an important step towards the development of such a theoretical framework, exploratory calculations have been made of the theoretical response, of relatively simple crystal models, to a variety of different modes of "large strain" loading. Results of such calculations, as are reviewed here, have exhibited a variety of interesting behaviours and thereby have provided insights into the nature of possible phenomena during homogeneous, large strain deformation of crystals. Possible modes of phase transformations have been suggested, and it has been demonstrated that computations of lattice behaviour at large strain can yield greater understanding of the bases for certain aspects of crystal elasticity in the reference, unloaded states [3]. These initial results also suggest that there remains much to be learned from future calculations, based upon relatively simple crystal models, for other modes of loading not yet fully explored.

An important consideration, relating to the

theoretical response of a crystal lattice to loading, is that of the “stability” of the loaded crystal and the nature of possible branching (from a primary path of deformation) associated with loss or exchange of stability. The problem of determining the stability limits (or the theoretical or ideal strength) of a perfect crystal is of fundamental interest because it is thought that the strengths of some metallic whiskers or fine filaments approach the theoretical limit. The problem is also relevant to our understanding of many phenomena occurring in the solid state; it plays an important role in determining the stress distribution near the tip of a crack and thus in determining whether a material will exhibit brittle or ductile behaviour [4, 5]. The definition of dislocation core radii [6, 7] and the loss of coherency occurring at particle–matrix interfaces [8–10] are also problems which involve large strain elasticity and the ideal strengths of crystals.

Macmillan [11] has given a comprehensive review on theoretical strengths of ideal crystals, including stability under load. However, since the appearance of Macmillan’s review article, recent work by Hill [2], Hill and Milstein [12], and Milstein and Hill [13–15] has led to major revisions in the methodology and principles of the assessment of crystal stability under load; in discussing theoretical crystal strength, the emphasis in the present review is thus on this more recent work.

2. General characteristics of various modes of loading

2.1. Qualitative features

As an example of the variety of phenomena and complexity of crystal response for a prescribed path of loading, we begin by mentioning some results of Huang *et al.* [16]. They computed the theoretical load–deformation behaviour of an initially fcc crystal subjected to shearing forces wherein the lattice parameters were unconstrained (i.e. as the crystal was deformed, all lattice parameters were varied in such a manner that the load remained parallel to the (100) planes and in the [010] direction* and that no other loading but this shear loading was present). This study was the first theoretical study of the unconstrained response of a crystal to such shear loading. Calculations were made of shear angle θ , lattice parameters, shear forces and stresses, and elastic moduli along the loading path. As a consequence

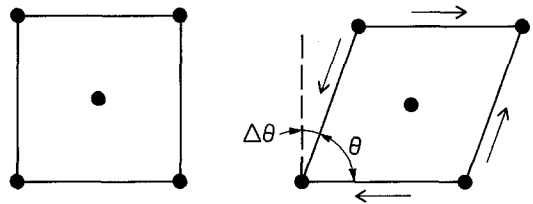


Figure 1 Side view of the fcc unit cell in the initial, unloaded fcc state (left) and under the applied shearing forces (right). For the prescribed state of loading, the value of θ could not be decreased beyond $\approx 82.4^\circ$ without the necessity of a first order lattice discontinuity.

of the fact that the calculations were for an “unconstrained” lattice, several unexpected results were obtained. For example, the shear angle θ (between the [100] and [010] directions), as well as all other lattice parameters, could be varied continuously up to a maximum critical variation occurring at $\Delta\theta \approx 7.6^\circ$; further continuous variation of θ required a first order transition (i.e. a discontinuity in the other lattice parameters) since a continuous path taking $\Delta\theta$ beyond $\approx 7.6^\circ$ did not exist! (There did exist a continuous path taking $\Delta\theta$ back to 0° , transforming the initial fcc structure into a bcc structure, and passing through a stress-free tetragonal structure on the way.) The crystal loading is indicated schematically in Fig. 1. The applied shear stress and internal energy versus θ are shown in Figs. 2 and 3. The crystal is initially in the unstressed fcc state A; a maximum stress is reached near C; the continuous path taking $\Delta\theta$ back to 0° (or θ back to 90°) is indicated as CDEFG, where E is the stress-free tetragonal state and G is the unstressed bcc state; the continuous increase in $\Delta\theta$ (or decrease in θ) beyond state D, while preserving the mode of loading, required the “discontinuous jump” from state D to state X. The computational techniques are reviewed briefly in what follows; for more detailed information, the reader is referred to the original literature.

In order to carry out actual calculations of load, strain, and elastic moduli, a crystal model is required whereby the internal energy W per atom or per unit cell can be expressed or calculated as a function of geometric variables q_r that define the state of homogeneous strain of the crystal:

$$W = W(q_1, q_2, \dots, q_6). \quad (1)$$

The most widely used approximation has been to

*The usual Miller index is employed. Thus in this example, the load is parallel to a “cube” face and to a “cube” edge of the (initially cubic) unit cell.

compute $2W$ by summing, over some 10^3 volume units of deformed crystal, the pairwise interaction energies associated with “bonds” on the representative atoms in one cell. Metals whose electronic structures are not too complex have been modelled by adding a volume-dependent contribution to the interionic energies [17]. In principle, one could also employ more sophisticated, mathematically complicated, rigorous (from a quantum mechanics viewpoint) crystal models, although at the present stage of development, it appears that much more can be learned from studies based upon the simpler, classical model of a crystal. It will, of course, be of great interest to “verify” some of the “classical” results using more sophisticated quantum models of crystals and particularly to perform computations with non-central forces so that Cauchy symmetry is not present. Work along these lines has been initiated by a group at Harvard University [18], where a first principles calculation of theoretical “tensile” stress of copper was recently made. (Actually the computations were for uniaxial elongation in a [100] direction and hence the state of loading was triaxial, such that the stresses in [010] and [001] were equal and apparently in tension.) From the viewpoint of assessing the validity of the various computations, it is satisfying to note that their theoretical results are in good agreement with analogous computations performed using the simpler central force. Morse model of a copper crystal [39].

In the pioneering work of Born and co-workers [19–25], the potential energy $\phi(r)$ between two atoms (in a crystal) separated by a distance r was taken to be of the “inverse power” or “Mie” form i.e.

$$\phi(r) = D \frac{nm}{n-m} \left[\frac{1}{n} \left(\frac{r_0}{r} \right)^n - \frac{1}{m} \left(\frac{r_0}{r} \right)^m \right], \quad (2)$$

where $n > m$. $d\phi/dr$ vanishes for $r = r_0$; $\phi(r_0) = -D$, the dissociation energy for a given pairwise “bond”; and D, n, m , and r_0 are empirical potential parameters determined from the experimental crystal properties (e.g. lattice parameter, compressibility, cohesive energy, etc., of the actual crystal). The particular case of $m = 6, n = 12$ is the “well known” Lennard–Jones function.

Born and co-workers used this model to study unloaded crystals with cubic [20] and rhombohedral [25] internal symmetry and loaded face centred crystals (initially cubic) subjected to [100] or “cube edge” uniaxial loading [21] and

hydrostatic tension and compression [23, 24]. In the absence of electronic computers, the numerical techniques for determining the required lattice summations were complicated and tedious [20–25]. This apparently is the reason why Born and Fürth limited their non-hydrostatic loading studies [21] to one example only, i.e. to the case of [100] uniaxial loading of an initially face centred cubic crystal with Lennard–Jones interatomic interactions. Nevertheless, the inverse power function, Equation 2, was the most mathematically tractable (among various types of two-body potential functions that could have been selected); although other functions, e.g. the Morse function,

$$\phi(r) = D \{ \exp [-2\alpha(r - r_0)] - 2 \exp [-\alpha(r - r_0)] \}, \quad (3)$$

had certain inherent theoretical advantages (see, for example, Girifalco and Weizer [26, 27]). With the advent of electronic computers, however, lattice summations of exponential functions could readily be performed. This led Milstein [28] to suggest a generalization of the Morse function, i.e.

$$\phi(r) = \frac{D}{m-1} \{ \exp [-m\alpha(r - r_0)] - m \exp [-\alpha(r - r_0)] \}. \quad (4)$$

D, α, r_0 , and m are empirical parameters; $d\phi/dr = 0$ at $r = r_0$; and $\phi(r_0) = -D$, the dissociation energy of two atoms. For the particular case of $m = 2$, Equations 3 and 4 are identical.

In [28], explicit functions $\phi(r)$, (Equation 4), were determined for a number of cubic crystals (from experimental values of the stress-free lattice parameter and elastic constants C_{11} and C_{12}) and the applicability (and limitations) of such a model was discussed. Subsequent studies [3, 16, 29–31], of the response of a crystal to selected modes of loading, employed the particular set of functions ϕ that were determined for the element nickel (Ni) for the reasons that: (i) among the fcc metals which were examined, Ni comes closest to obeying the Cauchy condition $C_{12} = C_{44}$; (ii) reasonably good agreement was obtained between theoretical and experimental pressure–volume relations in the region of anharmonic (i.e. non-linear) behaviour; (iii) the theoretical model exhibits a reasonably accurate stress–strain curve in the linear region (since experimental values of elastic moduli were used to determine the atomic parameters defining

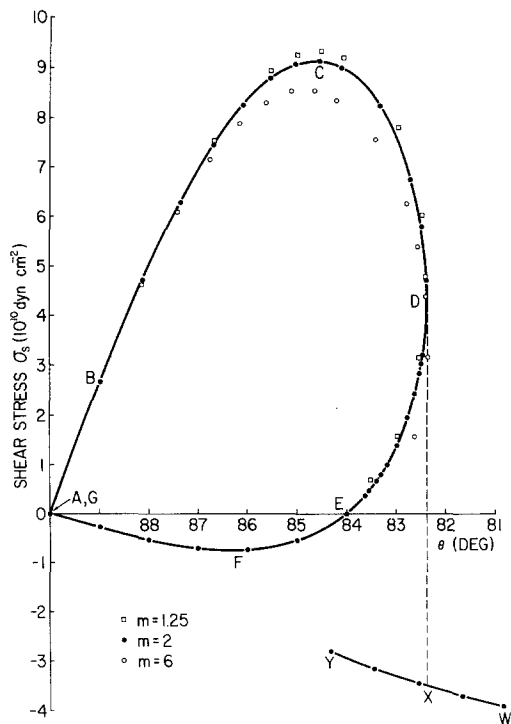


Figure 2 Theoretical values of applied shear stress σ_s calculated as a function of shear angle θ for the state of loading shown in Fig. 1 [16].

ϕ). Included in this set of functions ϕ were both short-range, steep functions and long-range, shallow functions. For example, in the “steepest” potential ϕ employed in the calculations (i.e. $m = 1,25$) about 92% of the cohesive energy per atom in the crystal comes from nearest-neighbour interactions and less than 0.1% from, say, all of the sixth- or seventh-neighbour interactions; whereas in the “shallowest” potential ($m = 6$), only about 51% of this cohesive energy can be attributed to nearest-neighbour interactions while as much as 3.1% comes from seventh-neighbour interactions. Nevertheless, the model was found to be self-consistent in the sense that the response of the crystal, even after very large strains, was found to be surprisingly insensitive to the details of the function ϕ (assuming, of course, that the same empirical data were used to specify each function ϕ in the set). For example, computations are shown in Fig. 2 for the cases $m = 1.25, 2$ and 6 in Equation 4.

As an interesting side comment, it is perhaps somewhat strange that the topic of the theoretical response of ideal crystals to loading remained rather dormant for more than 20 years after the original work by Born and co-workers. The present author first became interested in this topic in 1967

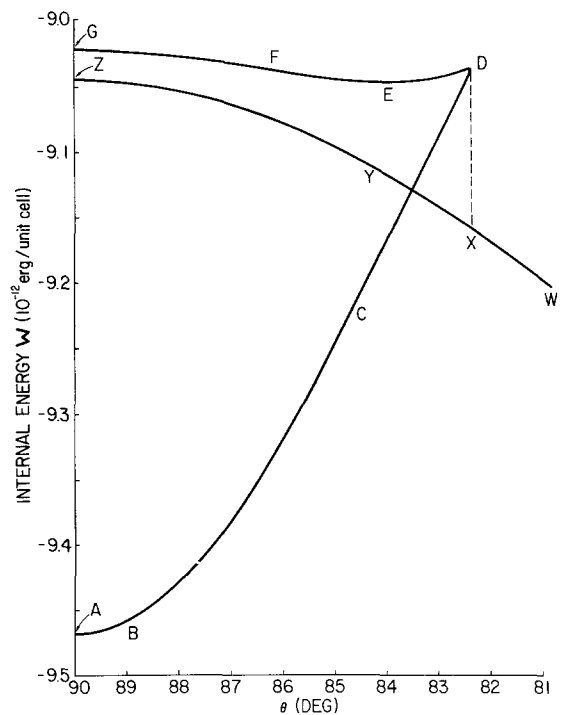


Figure 3 Internal energy W per unit fcc cell (i.e. per four atoms) versus shear angle θ , corresponding to the shear stress shown in Fig. 2 [16].

while he was a member of a Mechanics and Materials Group at RAND Corporation, Santa Monica, California, where there was considerable discussion regarding the possibility of using whiskers and fine filamentary single crystals as structural components. Milstein’s initial studies were for [100] uniaxial loading (i.e. cube-edge loading) of a body centred cubic lattice [32, 33] and face centred cubic lattices [29]. It soon became evident that for “large strain” loading, the path of load or stress versus the lattice parameter a_1 parallel to the load was essentially the same for either lattice type when subjected to unconstrained [100] uniaxial loading (i.e. at any stage along the loading path, the transverse lattice parameters ($a_2 = a_3$) are “adjusted” to ensure that the transverse loads are zero). The lattice structure is illustrated in Fig. 4, where it is readily seen that, under the prescribed loading programme, either a body centred tetragonal (bct) or a face centred tetragonal (fct) fundamental cell can be defined. It also then follows that the primary loading path passes through three zeros in general. That is, consider the fcc state to be stress free; under compression of the axial lattice parameter a_1 , the transverse fcc lattice parameters ($a_2 = a_3$) increase;

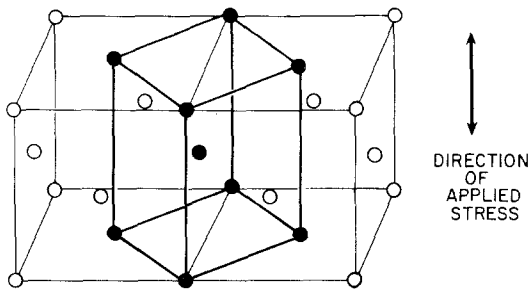


Figure 4 Two fundamental cells of the face centred tetragonal lattice with specific lattice sites shown with "solid" centres to indicate that the structure can also be considered as body centred tetragonal.

when the state $a_2 = \sqrt{2}a_1$ is reached, the body centred cell becomes cubic; since the transverse loads are zero, it follows from symmetry that the axial load is also zero in that state. Since the load must be tensile as $a_1 \rightarrow \infty$ and compressive as $a_1 \rightarrow 0$, the existence of two zeros on the primary loading path also implies a third zero, in general (although it is possible for only two zeros to occur in a special case where the load is tangent to the abscissa at the bcc state). Typical curves [29, 32, 33] of load or stress versus lattice parameter a_1 had the general appearance shown in Fig. 5. Generally, state c is at an energy minimum, b is at a local energy maximum, and a at a local minimum. The unstressed fcc state is at c . The unstressed bcc state was found at a for a lattice model of Fe [32, 33] and at b for Ni [29]; when the bcc state occurs at b it is unstable, since associated with a falling load characteristic, or equivalently a local maximum of strain energy. Additional special states at d , f , and e will be discussed shortly with relation to branching from the primary path under a programme of uniaxial loading.

With regard to the existence of the stress-free

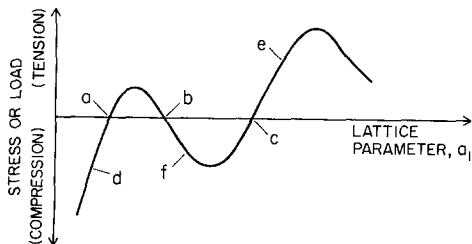


Figure 5 General behaviour of the load or stress versus axial lattice parameter for unconstrained [100] uniaxial loading of a body centred or face centred tetragonal lattice. State c is fcc (unstressed) and either state a or b is bcc (also unstressed).

tetragonal configuration (located at b in [32] and [33] and at a in [29]), the lattice structure in this state apparently is a tetragonal Bravais lattice without any higher symmetry. The same lattice configuration exists at E in Figs. 2 and 3. In passing, it is interesting to note that Born and co-workers were apparently of the opinion that the central force model of a crystal did *not* exhibit a stress-free tetragonal equilibrium state. This opinion apparently was based upon their study [21] of [100] uniaxial loading of a face centred cubic crystal and their additional calculations for unloaded rhombohedral lattices [25]. For example, in listing the significant results of his group's investigations of the behaviour of central force lattices, Born [34] includes the "result that tetragonal (non-cubic) Bravais lattices are not equilibrium configurations". However, apparently Born and Fürth *would have* seen the "equilibrium" (i.e. unstressed) tetragonal Bravais lattice under greater [100] lattice contraction; indeed, their theoretical load versus deformation curve did exhibit a minimum in compression (which, strangely, went unremarked).

Similar responses with triple zeros were noted for other uniaxial loadings. For the lattice model of nickel under [110] (i.e. face diagonal) load, Milstein and Huang [30] found the unstressed tetragonal state between two fcc states (equivalent but oriented differently). This behaviour is associated with a "branching" of the [100] and [110] paths, as will be discussed later. Milstein *et al.* [31] recently studied the theoretical mechanical behaviour of cubic crystals in unconstrained [111] (i.e. body diagonal) uniaxial loading. They demonstrated that a general axisymmetric loading path, of necessity, passes successively through three zeros where the lattice takes on the bcc , sc , and fcc configurations; based on that behaviour, a general proof was given that the unstressed sc lattice is always unstable (since it must occur in the central position, analogous to state b in Fig. 5).

Elastic moduli are central in theories of branching and instability. Thus, at this point, it is useful to review briefly the subject of elastic moduli of a crystal under load.

2.2 Elastic moduli

Homogeneous pure strain of a crystal is specifiable by any six parameters that define the geometry of the primitive or other fundamental cell. In con-

formity with the standard notation in Lagrangian mechanics, an arbitrary set of generalized co-ordinates or parameters can be denoted as q_r , $r = 1, \dots, 6$. Generalized conjugate variables are then defined by

$$p_r = \frac{\partial W}{\partial q_r}, \quad r = 1, \dots, 6, \quad (5)$$

where W is the internal energy of a (deformed) fundamental cell in the loaded crystal. A matrix of generalized elastic moduli can be defined as the array of coefficients in the relations between differential increments of the conjugate sets of variables;

$$dp_r = C_{rs}dq_s, \quad C_{rs} = \frac{\partial^2 W}{\partial q_r \partial q_s} \quad (6)$$

($r, s = 1, \dots, 6$; summation convention). The C_{rs} are dependent both on the level of strain and on the choice of generalized co-ordinates. However, when these are the elements of some strain measure, all such matrices coincide in the reference configuration itself, if it happens to be unstressed. In that case the C_{rs} are just conventional elastic moduli and the notation conforms with standard usage [12].

The three sets of geometrical variables q_r principally favoured in the literature are (i) the components of the Green's tensor (which were always adopted by the Born school), (ii) the components of the stretch tensor (which were introduced into lattice mechanics by Macmillan and Kelly [35, 36], and (iii) the Milstein or M variables (for $r = 1, 2, 3$, the q_r are the edges of the unit cell, and for $r = 4, 5, 6$, the q_r are the included angles). In principle, disregarding possible complexities of analysis, one could use the components of any other measure of strain as generalized co-ordinates. Hill [2] considered any tensor coaxial with the principal fibres and having principal values $f(\lambda_1)$, $f(\lambda_2)$, $f(\lambda_3)$, where $\lambda_1, \lambda_2, \lambda_3$ are the principal stretches; $f(\lambda)$ can be any smooth monotone function such that $f(1) = 0$, $f'(1) = 1$ (normalizations that ensure coincidence with the classical infinitesimal strain when the deformation is first order). Simple examples of $f(\lambda)$ are $\lambda - 1$, $\ln \lambda$, $(\lambda^2 - 1)/2$, the last of which generates the components of the Green's measure of strain. This topic is discussed in detail in [2] and [12].

Connections among various sets of moduli are given in [12] and [31] for particular paths of loading. For example, for an initially cubic crystal

subjected to a [100] uniaxial load l_1 (per unit reference cross-section), the transformations among the Green, stretch, and M moduli (C_{rs}^G , C_{rs}^S , and C_{rs}^M , respectively) are

$$\left. \begin{aligned} C_{11}^S &= \lambda_1^2 C_{11}^G + l_1/\lambda_1 \\ C_{22}^S &= \lambda_2^2 C_{22}^G \\ C_{12}^S &= \lambda_1 \lambda_2 C_{12}^G \\ C_{23}^S &= \lambda_2^2 C_{23}^G \\ C_{44}^S &= \lambda_2^2 C_{44}^G \\ C_{55}^S &= \frac{1}{4} \{ (\lambda_1 + \lambda_3)^2 C_{55}^G + l_1/\lambda_1 \} \end{aligned} \right\} \quad (7)$$

$$\left. \begin{aligned} \text{and } C_{rs}^M &= C_{rs}^S \text{ for } r, s \leq 3 \\ \text{with } C_{44}^M &= \lambda_2^4 C_{44}^G \text{ and } C_{55}^M = \lambda_1^2 \lambda_3^2 C_{55}^G, \end{aligned} \right\} \quad (8)$$

where λ_1 is the axial stretch (i.e. in the [100] direction) and $\lambda_2 = \lambda_3$ is the transverse stretch (i.e. in the [010] and [001] directions); by definition the stretch of any embedded fibre is the ratio of its final length divided by its initial length. The above formulae clearly demonstrate the dependence of the elastic moduli upon choice of geometric variables q_r , although for the "special case" $\lambda_1 = \lambda_2 = \lambda_3$ and $l_1 = 0$ (i.e. in the cubic reference state), $C_{rs}^G = C_{rs}^S = C_{rs}^M = C_{rs}$, i.e. the "usual" elastic moduli. Under the prescribed loading, the crystal is tetragonal so the symmetries $C_{22} = C_{33}$, $C_{12} = C_{13}$, and $C_{55} = C_{66}$ are maintained within any set of moduli (provided the principal axes are selected in a reasonable manner with regard to crystal symmetry).

2.3. Invariant path branchings

As noted by Hill and Milstein [12], "Branching of a primary path of deformation under a prescribed loading program, is well known to be closely associated with loss or exchange of stability . . . branching is . . . not coordinate invariant in general, when the criterion for its inception is stationarity of the conjugate forces during some virtual increment of deformation. On some paths, however, there are exceptional bifurcations that are substantially coordinate invariant on this criterion". Hill and Milstein [12] identified one such co-ordinate invariant bifurcation and examined it in detail. In view of the possible role of such bifurcations in any objective concept of ideal strength, special consideration is given to this topic here.

Consider the [100] loading path, as discussed above. Along this path, at the point at which $C_{22} = C_{23}$, there is a special "co-ordinate invariant" bifurcation. The bifurcation is co-ordinate invariant in the sense that it occurs at the same point on the primary path, irrespective of the choice of geometric variables or co-ordinates q_i used in specifying the strain and elastic moduli (assuming a "reasonable" choice with regard to lattice symmetry) [12]. When this state is reached, a bifurcation from the primary equilibrium (but not necessarily stable) loading path (on which the lattice possesses tetragonal symmetry) to a secondary equilibrium path (on which the lattice acquires orthorhombic symmetry) is possible under a programme of uniaxial load. By contrast, in general, as soon as a crystal departs from the tetragonal configuration that it assumes on the primary path of [100] uniaxial loading, additional loads will be present and thus the equilibrium loading becomes other than [100] uniaxial. However, at the "invariant eigenstate" $C_{22} = C_{23}$, the crystal *can* undergo a departure from tetragonal symmetry while maintaining the uniaxial [100] load. The nature of the bifurcation leading from the tetragonal to the orthorhombic path is as follows: all loads remain stationary (no loads act on the 1-2 or 1-3 faces of the cell and the uniaxial load normal to the 2-3 face remains *dead* [2]); the edges of the cell remain orthogonal; λ_1 remains stationary ($\delta\lambda_1 = 0$); and λ_2 and λ_3 vary according to $\delta\lambda_2 = -\delta\lambda_3$ (δ indicates an incremental change).

The invariant eigenstates $C_{22} = C_{23}$, relative to the face centred tetragonal cell, were found to occur in the region indicated by state e in Fig. 5 for lattice models of Ni [29] and Fe [33]; the $C_{22} = C_{23}$ states, relative to the body centred tetragonal cell, occurred in the regions of f for Ni [29] and d for Fe [33]. (The state $C_{22} = C_{23}$, relative to the f c t cell, occurs where $C_{44} = 0$, relative to the b c t cell, and vice versa; in [33] the computations were performed relative to the b c cell whereas in [29] the computations were based upon the f c cell.)

The path branching from state f (in Fig. 5) under uniaxial loading was studied in detail by Milstein and Huang [30] for the lattice model of Ni; they showed this path to be identical to the path of [100] (i.e. face diagonal) uniaxial loading of the f c c crystal. Furthermore, at the branching point, the Poisson ratios along principal directions normal to the load were of opposite algebraic

sign and *infinite* magnitude, and they remained of opposite sign along the full [110] path. Based upon the theoretical behaviour of the deformed crystal, Milstein and Huang [3] formulated the reasonably general hypothesis that, in [110] loading of an f c c crystal, the Poisson ratio in the [1 $\bar{1}$ 0] direction would be negative. The generality of this phenomenon was supported by an examination of the relevant Poisson ratios of a variety of f c c crystals, as computed from experimental values of elastic moduli C_{ij}^0 of the unstressed crystals. This is shown in Table I; references for the C_{ij}^0 data are given in [3]. It is important to note that, although the path-dependent computations were carried out within the framework of a particular lattice model, the qualitative theoretical behaviour apparently has fairly general applicability, as evidenced by the experimentally based results of Table I.

Fig. 6 shows the load and energy for the lattice model of Ni in [100] and [110] loading, as computed by Milstein and Huang [30]. In state A, the crystal is unstressed f c c; along path . . . ABCD, the crystal is in uniaxial load along a [110] direction (with respect to the axes of the face centred cell) and the symmetry of the crystal is orthorhombic (i.e. under [110] loading of an initially f c c crystal, a body centred orthorhombic cell can be identified). In state G, the crystal is also unstressed f c c (same as at A, but oriented differently); along path . . . FGHDIJ . . . , the crystal is in uniaxial load along a [100] direction (either with respect to the face centred or body centred cell axes) and the symmetry of the crystal is tetragonal. The invariant path branching at $C_{22} = C_{23}$ (relative to the b c cell) occurs at state D; the nature of the bifurcation is reviewed briefly, above, and is presented in great detail (including computations of the path-dependent elastic moduli) in [30].

The existence of the path branching discussed above evidently also affects the value of the theoretical maximum stress in [110] loading. For example, in unconstrained [100], [110], and [111] uniaxial loading, respectively, the same (initially) f c c crystal exhibits maximum theoretical values of stress of about 2.6, 0.9, and 2.6 (in 10^{11} dyn cm $^{-2}$) at axial stretches of about 1.25, 1.1, and 1.17 [29–31]. One might think, intuitively, that loading normal to a closer packed crystallographic plane (e.g. the [111] case) would yield a lower maximum theoretical tensile stress at

TABLE I Elastic constants C_{ij}^0 (in 10^{12} dyn cm $^{-2}$) and Poisson's ratios $\nu_{1\bar{1}0}$ and ν_{001} (as calculated from the C_{ij}^0) for fcc crystals (From Milstein and Huang [3])

Crystal	Temperature (K)	C_{11}^0	C_{12}^0	C_{44}^0	$\nu_{1\bar{1}0}$	ν_{001}
Pd	0	2.341	1.761	0.712	0.010	0.745
	50	2.336	1.768	0.707	0.005	0.753
	100	2.319	1.768	0.701	-0.004	0.765
	150	2.291	1.753	0.702	-0.015	0.777
	200	2.270	1.743	0.706	-0.028	0.789
	250	2.262	1.744	0.711	-0.038	0.801
	300	2.271	1.761	0.717	-0.049	0.813
Th	0	0.778	0.482	0.513	-0.215	0.753
	300	0.753	0.489	0.478	-0.223	0.794
Cu	0	1.762	1.249	0.818	-0.138	0.806
	300	1.684	1.214	0.754	-0.136	0.819
Ag	0	1.315	0.973	0.511	-0.093	0.809
	300	1.240	0.937	0.461	-0.096	0.828
Au	0	2.016	1.697	0.454	-0.029	0.867
	300	1.923	1.631	0.420	-0.032	0.876
Al	0	1.143	0.619	0.316	0.267	0.397
	300	1.068	0.607	0.282	0.272	0.414
Pb	0	0.555	0.454	0.194	-0.186	0.970
	300	0.495	0.423	0.149	-0.209	1.033
Ni	0	2.612	1.508	1.317	-0.051	0.607
	300	2.508	1.500	1.235	-0.055	0.631
Ne	4.7	0.0169	0.0097	0.0100	-0.13	0.65
	24.3	0.01175	0.0074	0.00595	-0.095	0.69
Ar	4	0.0411	0.0190	0.0210	0.006	0.459
	4.2	0.0367	0.0174	0.0234	-0.11	0.526
	82.3	0.0238	0.0156	0.0112	-0.083	0.710
Kr	0	0.0506	0.0287	0.0273	-0.078	0.611
Xe	151	0.0303	0.0190	0.0156	-0.10	0.69

a smaller value of axial stretch, since the closer the atomic packing within the plane, the greater the distance between successive planes. Comparison between the [100] and [111] cases tends to support such reasoning (although the maximum theoretical stresses are almost the same). The [110] case is clearly contrary to such "intuition", since the (110) planes are less closely packed than either the (100) or (111) planes; however, the anomalously low values of maximum [110] stress and corresponding stretch can be understood as a consequence of the (evidently) inherent branching of the [110] path from the [100] path, as shown in Fig. 6 and discussed above.

Computations have recently been carried out [40, 41] for the uniaxial loading paths branching from states d and e in Fig. 5, the latter of which corresponds with state F in Fig. 6.

A possible interesting connection between the

above results and experimental investigations of martensitic transformations might be mentioned. Gunton and Saunders [37] have associated the martensitic transformation (in indium and indium thallium alloys), from an fcc phase to a tetragonal phase, with a negative instability of the Poisson's ratio $\nu_{1\bar{1}0}$; i.e. $\nu_{1\bar{1}0}$ is negative in algebraic sign and as the transformation is approached, the magnitude of this negative quantity increases. In Milstein and Huang's computations, the stress-free tetragonal state was found along the equilibrium [110] uniaxial loading path at $\lambda_1 \approx 1.170$ (fairly close to the invariant $C_{22} = C_{23}$ state). However, in this case, the tetragonal structure was mechanically unstable.

3. Crystal stability under load

3.1. Relativity of the Born criteria

The first attempts to calculate the theoretical

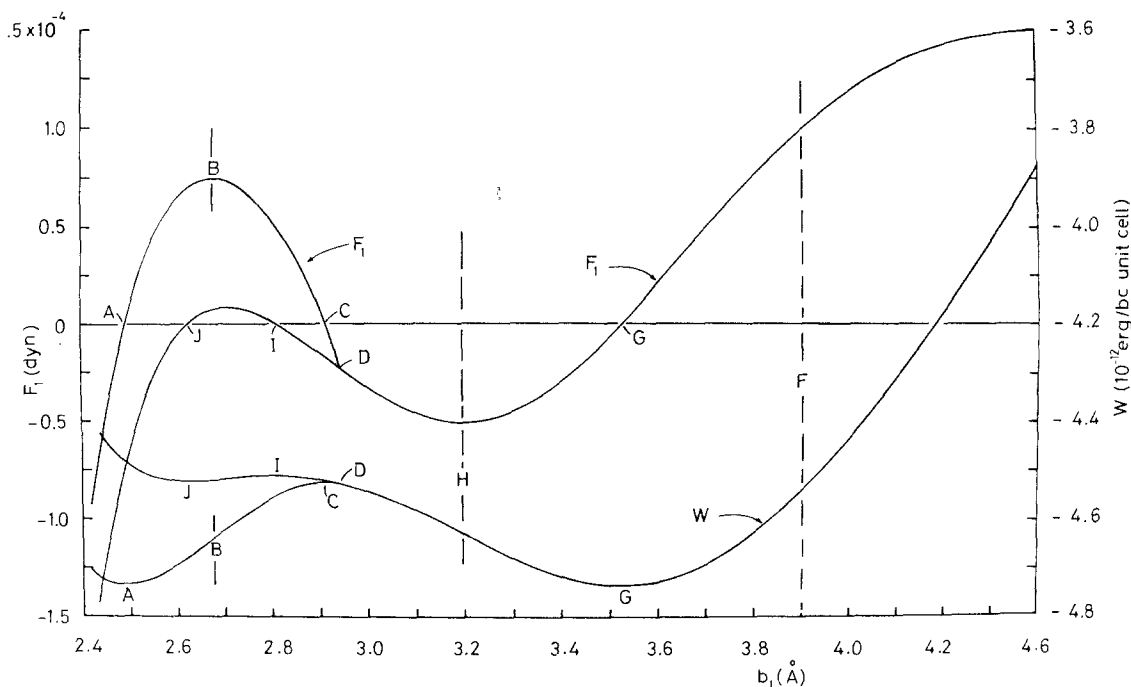


Figure 6 Energy per unit bc cell W and applied force F_1 acting on the face of the cell along two branches of the path of equilibrium for [100] uniaxial loading reckoned with respect to the bc cell axes. The lattice parameter b_1 is in the loading direction; at each stage, the transverse lattice parameters are "adjusted" to maintain *uniaxial* loading. Along branch . . . FGHIJ . . . the bc cell is tetragonal; along . . . ABCD, it is orthorhombic. (Also, when reckoned with respect to the fc cell axes, the branch . . . ABCD represents [110] uniaxial loading) [30].

response of a crystal to loading and to assess stability under load were carried out by Born and his co-workers [19–24]. In [19], Born presented the general principles that guided the work of his group. According to Born, any crystal capable of homogeneous deformation may be treated as a conservative dynamical system with six degrees of freedom; stability, in the ordinary Lagrangian sense was then to be assessed along conventional lines. The matrix of elastic moduli C_{rs} was to be examined for positive definiteness at each stage of loading, and the condition of passage from positive definite to semidefinite was to be taken as a "failure criterion" in assessing the ideal or theoretical strength of crystals. The condition that the above mentioned matrix be positive definite (popularly called the "Born stability criterion") is equivalent to the condition that the internal energy function W be locally strictly convex in its arguments (or that the Hessian matrix of W be positive definite) [12].

This criterion has been widely used in the literature in computations of theoretical crystal strengths as well as in applications to phase stability under hydrostatic pressure. However, as pointed

out by Hill [2], the Born criterion is not co-ordinate-independent. That is, for a crystal under load, the positive definiteness of the Hessian form $C_{rs}\delta q_r\delta q_s$ ($r, s = 1, 2, \dots, 6$; summation convention) is not independent of the choice of geometric variables q_r used in defining the strain. In addition (although not mentioned by Born), consistency of this notion of stability with the classical stability criterion requires a special environment in which the loads can be varied so as to "follow" the material during any disturbances and keep fixed the values of the conjugate forces, $\partial W/\partial q_r$, for the particular choice of generalized co-ordinates; these forces may consequently become different in kind from those in the configuration of equilibrium whose stability is under test. These matters are discussed in detail by Hill [2], Hill and Milstein [12, 15, 31], and Parry [38]. In practice, the Born school automatically took $q_r, r = 1, \dots, 6$, to be cartesian components of the Green measure of strain relative to the unloaded state, and there was no attempt to match the analysis to a practicable physical situation; the same can be said of all other choices in the literature.

The following quotation is taken directly from

Born [19] (Born's original notation is maintained, although the connection with notation used here should be clear): "If $\mathbf{a}_1, \mathbf{a}_2, \mathbf{a}_3$ are the vectors describing the cell we have to take as the molar parameters the six scalar products $\mathbf{a}_r \cdot \mathbf{a}_s = a_{rs}$ ($r, s = 1, 2, 3$) . . . The generalized forces corresponding to the molar parameters a_{rs} are the stress components $A_{rs} = -\partial A / \partial a_{rs}$ (1.5) which are determined by the external conditions (for instance, for a hydrostatic pressure $A_{11} = A_{22} = A_{33} = p$, $A_{23} = A_{31} = A_{12} = 0$). By solving these equations we find the equilibrium values of the a_{rs} (for instance, for a cubic cell $a_{11} = a_{22} = a_{33} = a^2$, $a_{23} = a_{31} = a_{12} = 0$). Not every solution is stable, but only those for which the quadratic terms in the expansion of A , with respect to small alterations δa_{rs} of the a_{rs} from their equilibrium values a_{rs}^0 , are positive definite. These terms have the form

$$A - A_0 = \frac{1}{2} \sum_{\substack{rs \\ \rho\sigma}} A_{rs,\rho\sigma}(T) \delta a_{rs} \delta a_{\rho\sigma},$$

$$A_{rs,\rho\sigma} = \left(\frac{\partial^2 A}{\partial a_{rs} \partial a_{\rho\sigma}} \right) \quad (1.6)$$

. . . If we now go to the limit of vanishing temperature, the free energy A becomes identical with the static potential energy U . But the stability conditions remain valid even in this limiting case where the thermodynamic system degenerates into a mechanical one. We must infer that the macroscopic stability of the lattice is determined by the positive definite character of the quadratic form (1.6) (where A is now replaced by U) of six variables only, the variations δa_{rs} of the cell parameters, . . .".

Born concluded [19] by stating: ". . . the calculation of the strength of crystals should be attacked by the method developed in this paper. This work will be carried out by my collaborators and pupils". In [21], Born and Fürth directly applied the Born stability criterion, as quoted above, to a crystal subjected to a particular mode of loading, i.e. [100] uniaxial. In [24], Fürth (as communicated by Born) employed the same criterion in a discussion of the stability of cubic crystals under hydrostatic pressure, i.e. "The stability condition for a cubic lattice under uniform stress in the direction of one of the axes (Born and Fürth, 1940) can easily be transformed into the stability conditions for a uniform pressure p in all directions. We have only to assume that the atomic distances are equal for all three axes, that is, the con-

stant c introduced in (Born and Fürth, 1940) is equal to b , and . . . replace the equilibrium conditions (12) of that paper by the conditions $F_i^0(b, b, b) = p/2a^2$ ($i = 1, 2, 3$) where a is the lattice constant for zero pressure".

In discussing this view of crystal stability, Hill and Milstein [12] wrote: ". . . it is in the detail of this theory that different writers have in practice diverged by virtue of choosing different sets of generalized coordinates. This is important because, in a crystal under load, convexity of the internal-energy function is not coordinate invariant Consequential divergences in estimates of strength previously escaped notice since atomic bonds were at the same time differently modeled by the respective writers . . .". Hill and Milstein introduced the terms M strength, G strength, and S strength to indicate the ranges of deformation over which the respective Hessian forms $C_{rs} \delta q_r \delta q_s$ remain positive definite (for M , G , and S variables). They then illustrated qualitative divergences, with the aid of some general comparison theorems that they developed. For example, in the pioneering investigation by Born and Fürth [21], an initially face centred cubic lattice was loaded uniaxially in a cubic direction ($q_1 \neq q_2 = q_3$ and the cell edges remain orthogonal; the q_i are "adjusted" so that the loading is uniaxial). A Lennard-Jones model was adopted and the G strengths were computed for both tension and compression. In neither case was the critical variation (causing the semi-definite Hessian to vanish) described explicitly; it may be inferred that in tension it would be $\delta \lambda_1 = 0, \delta \lambda_2 = -\delta \lambda_3 \neq 0$, coaxial with the basis, while in compression it would be the *actual* $\delta \lambda_{ij}$ at the algebraic minimum of the Green's conjugate stress l_1/λ_1 . With the aid of the comparison theorems, Hill and Milstein [12] concluded that, for Born and Fürth's crystal, in tension the G strength, M strength, and S strength are all equal, but in compression the G strength is the greatest. More recently, Macmillan and Kelly [35, 36] computed the S strengths of sodium chloride (Born-Mayer model) and argon (Lennard-Jones model). The reference basis and configuration are the cubic axes of the experimentally observed (and theoretically stable) structures at zero stress and temperature. Three paths of deformation are followed: (i) uniaxial extension with $\lambda_1 > 1, \lambda_2 = \lambda_3 = 1$; (ii) uniaxial extension with $l_1 > 0, l_2 = l_3 = 0$; (iii) plane dilatation with $\lambda_1 = 1, \lambda_2 = \lambda_3 > 1$. All three loads remain tensile along the path segments (ii) and (iii). With the aid

of their comparison theorems, Hill and Milstein [12] were able to demonstrate that the critical variations in (i), (ii), and (iii) for sodium chloride and in (iii) for argon were such that “the G strength is certainly less than the S strength”, but they were unable to otherwise sharpen the comparison. For argon, the critical variation for (i) was not reported, while for (ii), the critical variation was such that comparisons among the G , M , and S strengths could not “be sharpened”.

Other qualitative examples can be found in [12]. However, at the time of their 1977 paper [12], Hill and Milstein noted that “Whether convexity of the energy has a strong or a weak dependence on any reasonable choices of the geometric variables remains to be investigated . . .”. Since then, detailed computations of the domains of Born stability have been carried out for cubic crystals subjected to [100] [42], [111] [31] and hydrostatic [13–15] loading, for the cases of G , S , and M variables. For the uniaxial loadings, the ranges of Born stability were found to be relatively insensitive to choice of strain variables (at least for the particular choices employed). However, interesting and significant qualitative and quantitative divergences were found for the case of hydrostatic loading, as is discussed in the following section.

3.2. Hydrostatic loading

The classical Lagrange–Dirichlet criterion for elastic stability, when applied to a cubic crystal under a hydrostatic pressure P that does not vary during any departure from a considered configuration of equilibrium, gives

$$\kappa(P) > 0, \quad \mu(P) > 0, \quad \mu'(P) > 0, \quad (9)$$

as shown briefly in [12]. Here κ is the bulk modulus, while μ and μ' are the usual shear moduli in the relation between the cubic-axes components of the Cauchy stress increment $\delta\sigma_{ij}$ and the rotationless strain increment $\delta\epsilon_{ij}$ (reckoned relative to the *current* configuration under P). A fully rigorous derivation of Conditions 9 via the modern theory of bifurcation for elastic continua is presented in [15]. The treatment and subsequent stability criterion, Condition 9, is classical in that (i) the loading environment is fully specified, to sufficient order and in both its active and passive modes, and (ii) the potential energy of the system as a whole is examined in all the nearby, possibly inhomogeneous, configurations allowed by the kinematic constraints, if any. This criterion is therefore dis-

tinguished from the “notional” criterion of Born, as discussed in the prior section.

In an extensive three part series of papers, Milstein and Hill [13–15] reported computations of the bulk and shear moduli of the entire Morse-model family of fcc, bcc, and sc monatomic crystals under arbitrary fluid pressure. The computations were extended to dilatations, up to magnitudes where the lattice cohesion would in practice be lost. (It is well known that states of pure hydrostatic tension can be approached locally near cracks and other stress-raisers. Since controlled experimentation with this type of loading is fraught with difficulties, a special significance attaches to the theoretical moduli.) The stable range of each lattice as well as the potential bifurcations at the range limits were presented and discussed in terms of the role of the particular lattice structure and the effective range of the interatomic potential function as specified by the parameter $\beta \equiv e^{a/r_0}$ (see Equation 3); larger β means shorter range and steeper functions ϕ (see Fig. 2 in [13]).

The fcc lattices were found to be stable in com-

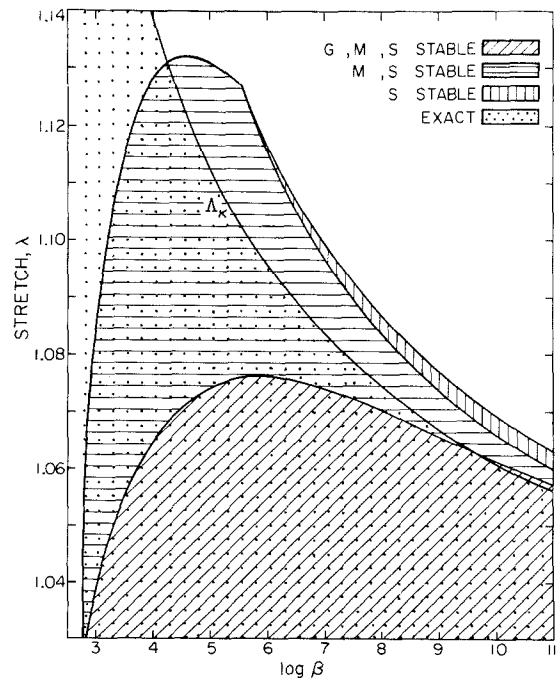


Figure 7 Regions of notional stability according to the Born criterion, Conditions 10, relative to the G , M , and S variables (indicated as G , M , and S stable, respectively) and stability in a hydrostatic environment (indicated as “EXACT”) for the Morse family of monatomic face centred cubic crystals [15].

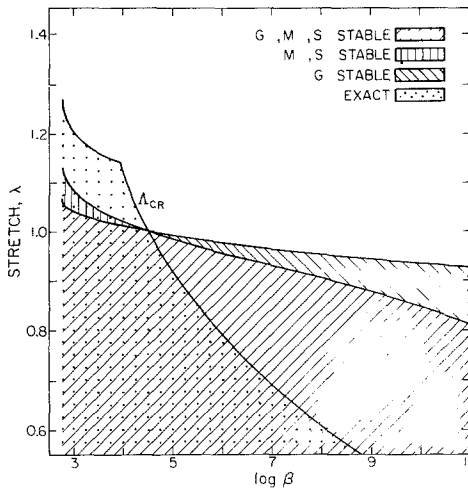


Figure 8 Regions of notional stability according to the Born criterion, Conditions 10, relative to the G , M , and S variables (indicated as G , M , and S stable, respectively) and stability in a hydrostatic environment (indicated as "EXACT") for the Morse family of monatomic body centred cubic crystals [15].

pression and in tension up to an all round stretch $\lambda = \Lambda_{\kappa}$, at which point the bulk modulus vanishes; Λ_{κ} is a monotonically decreasing function of $\log \beta$. The bcc lattices are stable for $\lambda < \Lambda_{\text{CR}}$, where the bulk modulus or the shear modulus μ vanishes (depending upon the value of $\log \beta$) at $\lambda = \Lambda_{\text{CR}}$. For very large values of $\log \beta$, a second range of bcc stability is located in a region of hydrostatic expansion. The sc crystals are stable only in a range of hydrostatic tension and only for relatively short-range interatomic interactions (large $\log \beta$); Milstein and Hill's study apparently is the first in which a theoretical range of stability of sc crystals has been revealed.

In contrast with the classical criterion for cubic crystals under hydrostatic loading, Conditions 9, the Born criterion leads to

$$C_{11} + 2C_{12} > 0, \quad C_{11} - C_{12} > 0, \quad C_{44} > 0. \quad (10)$$

At zero load Conditions 9 and 10 are naturally equivalent, but when $P \neq 0$, they predict different domains of stability; moreover, Conditions 10 are thoroughly "relative" in the sense that they are dependent on the choice of generalized co-ordinates, since, as noted in the previous section, the convexity of W is not co-ordinate-invariant under load [2]. Furthermore, the Born criterion, Conditions 10, evidently is not equivalent to the classical criterion, Conditions 9, for any choice of strain variables q_r for a cubic crystal under constant hydrostatic loading. (It is emphasized, in this discussion, that, in general, the bulk and shear moduli of Conditions 9, as well as the elastic moduli $C_{rs} \equiv \partial^2 W / \partial q_r \partial q_s$ of Conditions 10, are the moduli appropriate to the "strained lattice" in its *current* state of hydrostatic loading.)

Milstein and Hill [15] also examined the consequences of attempting to assess stability of the Morse function fcc, bcc, and sc cubic crystals under hydrostatic loading via the "simplistic notion" expressed in Conditions 10 for the cases in which the elastic constants are evaluated relative to the G , M and S variables. The respective regions of convexity (i.e. the regions over which the Born criterion (Conditions 10) is satisfied for the respective choices of strain variables) are called the regions of G , M , and S stability. In order to distinguish these regions from those of classical stab-

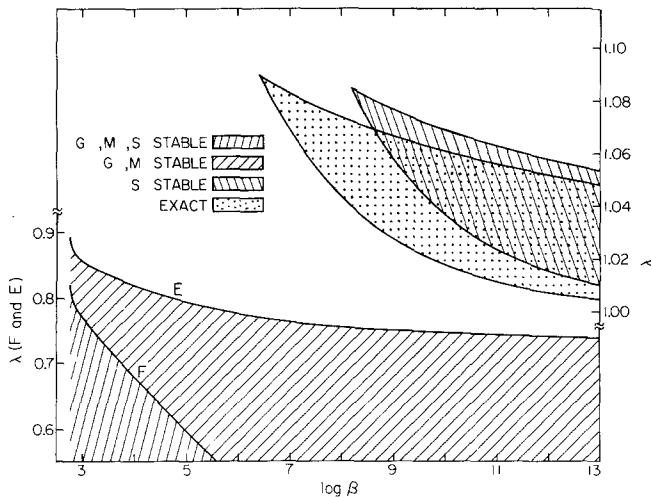


Figure 9 Regions of notional stability according to the Born criterion, Conditions 10, relative to the G , M , and S variables (indicated as G , M , and S stable, respectively) and stability in a hydrostatic environment (indicated as "EXACT") for the Morse family of monatomic simple cubic crystals [15].

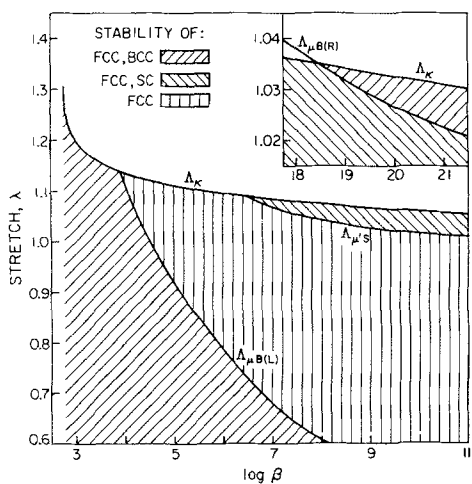


Figure 10 Ranges of stability of the three cubic lattices for the Morse model family of fcc, bcc, and sc monatomic crystals under constant hydrostatic loading [15]. (The region in the upper "insert" indicating stability of fcc and bcc below Λ_K and above $\Lambda_{\mu B(R)}$ is also sc-stable).

ility in a hydrostatic environment according to Conditions 9, the terminology "exact" is applied to the latter. Here it might be emphasized that the popular belief apparently is that the Born criterion is a useful and correct way to assess elastic stability under hydrostatic pressure. However, the results of Milstein and Hill, as summarized in Figs. 7 to 9, clearly demonstrate that significant qualitative discrepancies occur when this criterion is employed. The current volume per atom is $\lambda^3 V$, where V is the volume per atom when $P = 0$ and λ is the all-round stretch. For each lattice the range of classical (as well as Born) stability depends uniquely on the value of $\log \beta$ [13–15]. The computations were made within the framework of a crystal model that is both mathematically tractable and sufficiently realistic for the intended purpose; values of $\log \beta$, calculated from experimental data, vary from about 3 to 8 [26, 28].

Finally, the classical ranges of stability for all three lattices are summarized in Fig. 10.

Acknowledgement

This work was supported by the US National Science Foundation under Grant no. DMR78-06865.

References

1. R. H. SNOW, *Powder Technol.* **13** (1974) 33.
2. R. HILL, *Math. Proc. Cambridge Phil. Soc.* **77** (1975) 225.

3. F. MILSTEIN and K. HUANG, *Phys. Rev. B* **19** (1979) 2030.
4. A. KELLY, "Strong Solids" (Clarendon, Oxford, 1966).
5. A. KELLY, W. R. TYSON and A. A. COTTRELL, *Phil. Mag.* **15** (1967) 567.
6. P. C. GEHLEN, A. R. ROSENFELD and G. T. HAHN, *J. Appl. Phys.* **39** (1968) 5246.
7. Z. S. BASINSKI, M. S. DUESBERY and R. TAYLOR, *Phil. Mag.* **21** (1970) 1201.
8. M. F. ASHBY, S. H. GELLES and L. E. TANNER, *ibid.* **19** (1969) 757.
9. L. M. BROWN, G. R. WOOLHOUSE and U. VALDRE, *ibid.* **17** (1968) 781.
10. L. M. BROWN and G. R. WOOLHOUSE, *ibid.* **21** (1970) 329.
11. N. H. MACMILLAN, *J. Mater. Sci.* **7** (1972) 239.
12. R. HILL and F. MILSTEIN, *Phys. Rev. B* **15** (1977) 3087.
13. F. MILSTEIN and R. HILL, *J. Mech. Phys. Solids* **25** (1977) 457.
14. *Idem*, *ibid.* **26** (1978) 213.
15. *Idem*, *ibid.* **27** (1979) 215; F. MILSTEIN and R. HILL, *Phys. Rev. Lett.* **43** (1979) 1411.
16. K. HUANG, F. MILSTEIN and J. A. BALDWIN, Jr, *Phys. Rev. B* **10** (1974) 3635.
17. Z. S. BASINSKI, M. S. DUESBUERY and R. TAYLOR, Proceedings of the Second International Conference on Strength of Metals and Alloys, Vol. 1 (American Society for Metals, Cleveland, 1971) p. 118.
18. E. ESPOSITO, A. E. CARLSSON, D. D. LING, H. EHRENREICH and C. D. GELATT, Jr, *Philosophical Magazine*, in press.
19. M. BORN, *Proc. Cambridge Phil. Soc.* **36** (1940) 160.
20. R. D. MISRA, *ibid.* **36** (1940) 173.
21. M. BORN and R. FÜRTH, *ibid.* **36** (1940) 454.
22. M. BORN and R. D. MISRA, *ibid.* **36** (1940) 466.
23. R. FÜRTH, *ibid.* **37** (1941) 34.
24. *Idem*, *ibid.* **37** (1941) 177.
25. H. W. PENG and S. C. POWER, *ibid.* **38** (1942) 67.
26. L. A. GIRIFALCO and V. G. WEIZER, *Phys. Rev.* **114** (1959) 687.
27. *Idem*, National Aeronautics and Space Administration Technical Report R-5 (1959).
28. F. MILSTEIN, *J. Appl. Phys.* **44** (1973) 3825.
29. *Idem*, *ibid.* **44** (1973) 3833.
30. F. MILSTEIN and K. HUANG, *Phys. Rev. B* **18** (1978) 2529.
31. F. MILSTEIN, R. HILL and K. HUANG, *Phys. Rev. B.*, in press.
32. F. MILSTEIN, "Theoretical Strength of Perfect Crystalline Materials", prepared for United States Air Force Project RAND, RM-6379-PR (1970).
33. F. MILSTEIN, *Phys. Rev. B* **3** (1971) 1130.
34. M. BORN, *Proc. Cambridge Phil. Soc.* **39** (1943) 100.
35. N. H. MACMILLAN and A. KELLY, *Proc. Roy. Soc. Ser. A* **330** (1972) 291.
36. *Idem*, *ibid.* **330** (1972) 309.
37. D. J. GUNTON and G. A. SAUNDERS, *Proc. Roy. Soc. London A* **343** (1975) 63.
38. G. P. PARRY, *Q. J. Mech. Appl. Math.* **31** (1978) 1.

39. F. MILSTEIN and B. FARBER, *Philosophical magazine*, in press.
40. F. MILSTEIN and B. FARBER, *Phys. Rev. Lett.* (1980), in press.
41. F. MILSTEIN, R. HILL and B. FARBER, unpublished work.
42. F. MILSTEIN and B. FARBER, unpublished work.

Received 12 September and accepted 3 October 1979.